Sampling the intramyocellular triglycerides from skeletal muscle

Zengkui Guo,[1,*] Prasanna Mishra,[†] and Slobodan Macura[†]

Endocrine Research Unit* and Mayo NMR Facility,[†] Mayo Foundation, Rochester, MN 55905

Abstract **To determine the extent and microanatomical distribution of extramyocellular adipocytes associated with skeletal muscle, histological, biochemical, nuclear magnetic resonance proton spectroscopic and microcomputed tomography techniques were employed to analyze skeletal muscle samples from lean and obese Sprague-Dawley rats. Significant amounts of extramyocellular adipocytes were found on the exterior surface of rat gastrocnemius, soleus, and tibialis anterior muscles. The triglyceride content of these exterior adipocytes in these muscle groups was 2- to 3-fold greater than that of the respective intramyocellular triglyceride pool ($P = 0.01$). Thus, the exterior adipocytes associated with skeletal muscle samples are an abundant source of extramyocellular fat potentially contaminating the intramyocellular triglyceride pool if not carefully and completely removed. On the other hand, no adipocytes were found in the interfascicular space (between muscle bundles) or the intrafascicular space (between muscle fibers) in any of the three rat muscles. The feasibility of and procedures for removing extramyocellular fat by microdissection techniques to obtain pure muscle sample were also evaluated. Complete removal of the extramyocellular adipocytes from rat skeletal muscle, using microdissection with a stereo microscope, was found to be practical and effective. It is concluded that pure muscle samples free of contamination by extramyocellular fat can be obtained, but only if microdissection techniques are utilized.**—Guo, Z., P. Mishra, and S. Macura. **Sampling the intramyocellular triglycerides from skeletal muscle.** ***J. Lipid Res.*** **2001.** 42: **1041–1048.**

Supplementary key words intracellular • extracellular • human • rat

Intramyocellular triglyceride (imcTG) content in the skeletal muscle is strongly correlated with insulin resistance in human obesity and diabetes (1–3). However, the metabolism of imcTG is poorly understood. A major reason for this is the difficulties associated with the sampling of the true intramyocellular lipid pools. Because muscle may contain adipocytes (4, 5), the feasibility of sampling the pure imcTG pool without contamination by the extramyocellular triglycerides (emcTG) has been questioned. Some investigators believe that skeletal muscle contains adipose tissue that cannot be removed or separated from muscle fibers, making it difficult, if not impossible, to sample the true intramyocellular lipids. The high variability of the reported imcTG content highlights this possibility (6–8). The high variability suggests that the imcTG pool had been contaminated to varying degrees by extramyocellular fat.

Because the metabolism of adipocyte TG is likely fundamentally different from that of imcTG, and the pool size of imcTG in skeletal muscle is characteristically small (6, 9), contamination by the more abundant extramyocellular sources would seriously confound the results obtained from imcTG metabolic studies. Therefore, the ability to separate and remove emcTG from muscle samples is a limiting factor in the investigation of imcTG metabolism. Given our interest in this field, we elected to directly examine this issue in the rat, a species that has been heavily used in the studies of skeletal muscle lipid metabolism. We hypothesized that skeletal muscle-associated adipocytes exist only between muscle groups but not between muscle fibers and therefore are removable by appropriate techniques. The goals of this study were to evaluate the degree and the anatomic location of extramyocellular adipocytes associated with rat skeletal muscle, using histological, biochemical, NMR spectroscopic, and microcomputed tomography (micro-CT) techniques, and to evaluate the feasibility of and procedures for removing the extramyocellular adipocytes.

MATERIALS AND METHODS

Animals

Male Sprague-Dawley rats were fed either regular rat chow (lean, 400–500 g) or a 55% high fat diet (obese, 550–650 g) ad libitum. Before the study, the rats were fasted overnight. The next morning, the rats were anesthetized intravenously with sodium pentobarbital (60 mg/kg) and muscle samples were taken from gastrocnemius, soleus, and tibialis anterior muscles. The muscle samples were rinsed in cold saline and stored at −80°C for later analysis.

Abbreviations: emcTG, extramyocellular triglycerides; imcTG, intramyocellular triglycerides.

[1] To whom correspondence should be addressed.
e-mail: guo.zengkui@mayo.edu

Histological examination of skeletal muscle

The frozen muscle samples were thawed and examined under a dual-lens stereo microscope with a power of ×8–50 (SMZ-2B; Nikon, Japan). Most of the examinations were performed with a power of ×10–20 magnification so that the individual fat cells are readily identifiable and visible. Under the microscope, adipocytes identified on the muscle were removed with surgical instruments. The major internal blood vessels, along with the associated fascia and any adipocytes, were dissected carefully. The interfascicular spaces (between muscle bundles) were then searched thoroughly for adipocytes. The images of the muscle tissue and the identified adipocytes, before and after the microdissection, were recorded with a 35-mm Olympus camera mounted on the stereo microscope. An adjustable dual-light illuminator provided the illumination. Some of the muscle samples were cross-sectioned (6–10 μm in thickness) for Oil Red O staining at the Mayo Histology Laboratory. The slides were viewed under a high resolution light microscope (Axiophot; Zeiss, Germany) and the image was recorded with a 35-mm camera.

Biochemical examination

All identified adipose tissue and adipocytes associated with muscle (interior and exterior) and the internal blood vessels were dissected thoroughly under the stereo microscope (dissected). These samples were then rinsed thoroughly in cold saline until free of floating lipid droplets. For comparison purposes, an aliquot of each muscle sample was not subjected to such extensive dissection; rather, only the grossly visible exterior adipocytes or fat tissue was removed (not dissected). Both the dissected and nondissected muscle samples were extracted for total lipids by the method of Folch, Lees, and Sloane-Standley (10), and TG was purified by HPLC (11) and quantitated by an enzymatic method (12).

NMR proton spectroscopy

^{1}H NMR spectroscopic analyses were performed on a Bruker AMX500 spectrometer operating at 500 MHz (all at 25°C). Each muscle sample was dissected free of exterior fat and immersed in deuterated water in an NMR tube (5 × 180 mm, soleus; 10 × 180 mm, gastrocnemius and tibialis anterior) with the orientation of the fibers parallel to the magnetic field. The samples were scanned 100–400 times in spin and nonspin mode. The observed chemical shifts of the methylene group protons of TG fatty acids were calibrated during each analysis against the water peak artificially set at 4.8 ppm. The lower detection limit of the proton spectroscopy NMR was determined with vegetable oil dissolved in deuterated chloroform ($CDCl_3$) at concentrations of 480, 48, and 12 μmol.

Micro-CT

Soleus muscles from lean and obese rats were used for detection of adipocytes in skeletal muscle. The muscle samples were first fixed by formalin, followed by dehydration with 70%, 80%, 95%, and 100% ethanol consecutively, and finally clearing with HistoClear (National Diagnostics, Atlanta, GA). The muscle was then embedded in paraffin for X-ray micro-CT analysis. The final length of the muscle samples was significantly shorter than that of the original, fresh tissue as a result of shrinking on muscle biopsy and dehydration. The analysis was performed on an X-ray micro-CT scanner, which scanned the embedded muscle sample every 6 μm, resulting in more than 500 muscle slices scanned. The images from these scans were digitized and stored in a micro-PC. The stored images were then tomographically reconstructed, in the original order, to create a global, maximum intensity projection image of the entire muscle sample. The global image can be viewed at any angle as desired. If a fat cell is present within the muscle sample, a darker, round-shaped spot should be visible against the gray background because less dense materials such as fat cells absorb less X-ray than does the more dense muscle tissue. More detailed instrumental operation and analytical procedures with X-ray micro-CT scanner are described in a previous publication (13).

RESULTS

Gross histology

Figures 1 and **2** show exterior images of a soleus muscle and part of a gastrocnemius muscle from an obese rat before microdissection.

Adipocytes were usually observed on the exterior of soleus muscle on the surface of the myotendon junction, either scattered or as a thin layer of adipocytes (A in Fig. 1). These adipocytes were not visible to the naked eye, requiring the use of a microscope. On occasion, small aggregates of adipocytes were associated with the epimysium (indicated by the arrow in Fig. 1 and in **Fig. 3B**). Characteristically, two branches of blood vessel enter the soleus (Fig. 1). At this site, adipocyte aggregates were often present (arrow, Fig. 3B). The vessels extend into the muscle body, where they are often associated with adipocytes in the area near the entry site (arrow, Fig. 3A). These internal blood vessels can be readily identified and removed under a microscope (Fig. 3B). On the inside, except for the blood vessels and the fascia (perimysium and endomysium), soleus muscle contains only clean muscle fascicles. Each of the fascicles in turn contains varying numbers of muscle fibers (F in Fig. 3A and 3B). Careful examination of the individual fascicles revealed that the interfiber interface (the interstitial space) did not contain adipocytes

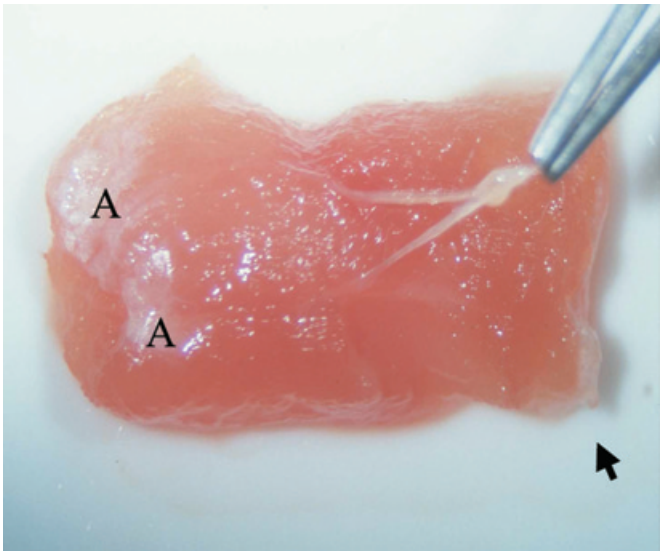

Fig. 1. Image of a soleus muscle from a high fat-induced obese rat. Notice the muscle had shrunk in length after its removal from the rat. Two branches of a blood vessel characteristically enter the muscle. Numerous adipocytes (A) are seen on the surface of the myotendon junction at the end. Aggregates of adipocytes can be found at the lateral side (arrow). Original magnification: ~×8.

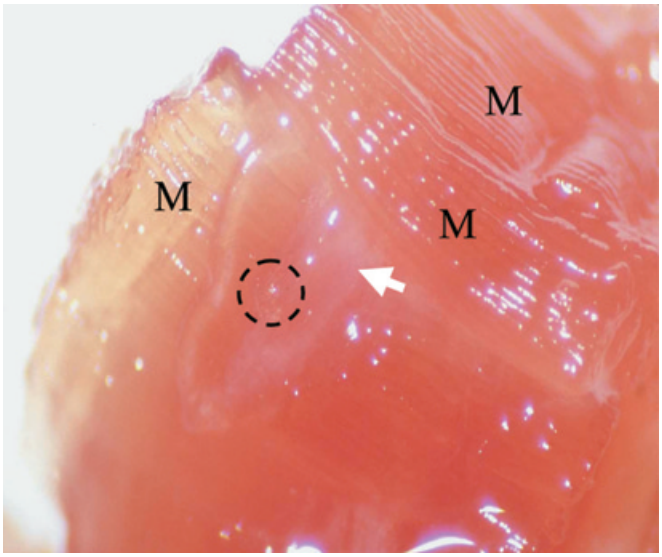

Fig. 2. Image of a gastrocnemius muscle (partial) from a lean rat before removal of exterior adipocytes. Muscle fascicles containing clean muscle fibers (M) are clearly visible. A blood vessel (arrow) enters the muscle between two muscle fascicles. An aggregate of adipocytes is associated with the vessel (dashed circle). Original magnification: ~×15.

(**Fig. 4**), nor did the interfascicular space (between muscle bundles), in lean or obese rats.

Aggregates of adipocytes were often present on the surface of the gastrocnemius (dashed circle in Fig. 2) in association with blood vessels (arrow, Fig. 2) at the point at which they enter the muscle. Again, the internal vessels were readily identifiable and removable under a microscope (**Fig. 5**). After such removal, gastrocnemius contained only clean fascicles that contained no adipocytes between the fibers (M in Fig. 2). Like the soleus muscle, no adipocytes were detected in the interfascicular space.

The tibialis anterior muscle is completely covered by a dense white fascia that was always removed during the muscle biopsy. As with the other two rat muscle types (described above), no inter- or intrafascicular adipocytes were detected. Intramuscular vessels between the fascicles were easily removed. Usually, the tibialis anterior and gastrocnemius muscles had fewer internal blood vessels than the soleus. These two muscle types also had fewer adipocytes on the surface compared with the soleus.

Histological examination of extramyocellular adipocytes

Six rat soleus and gastrocnemius muscle samples were thoroughly dissected free of adipocytes as described above and used to make 36 cross-sectional slides. To increase the chance of observing adipocytes, slides spaced a relatively great distance apart (100–200 μm) were used. The slides were stained with Oil Red O (specifically for neutral lipids) and examined under a high resolution light microscope (Labophot 2; Nikon). A representative image from each muscle is shown in **Fig. 6**. The images show that some fibers contained large lipid droplets that were readily visible whereas others did not show such lipid droplets. However, no adipocytes or TG were detected between muscle fibers (Fig. 6A and 6B).

TG content of skeletal muscles

Samples of the three rat skeletal muscles were thoroughly dissected free of all external adipocytes and major internal blood vessels under a stereo microscope. The TG content of the muscles after the microdissection was ap-

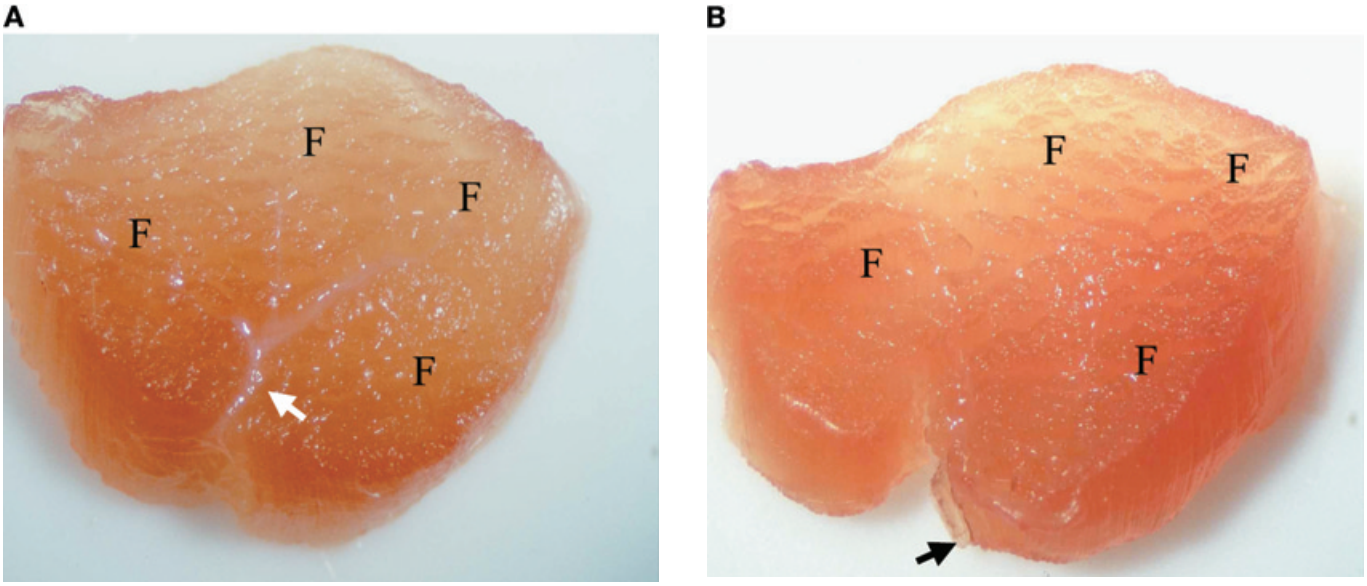

Fig. 3. A: A slice of soleus muscle from an obese rat. The image shows a major internal blood vessel and its branches. Major vessels are often associated with adipocytes at the entry area. As the vessel branches into the muscle, fewer adipocytes can be found. Note the blood vessel is white in color, which does not necessarily indicate it is fat tissue. The muscle slide contains many clean fascicles (F). B: The same sample as in (A) but with the blood vessels removed. The muscle now contains only fascicles (F) within which individual fibers are visible. The slide is manipulated in order to expose the clean interfascicular space (without adipocytes). A piece of adipose tissue at the blood vessel entry point (arrow) is purposely left to show the area where fat tissue is seen often. Original magnification: ~×10.

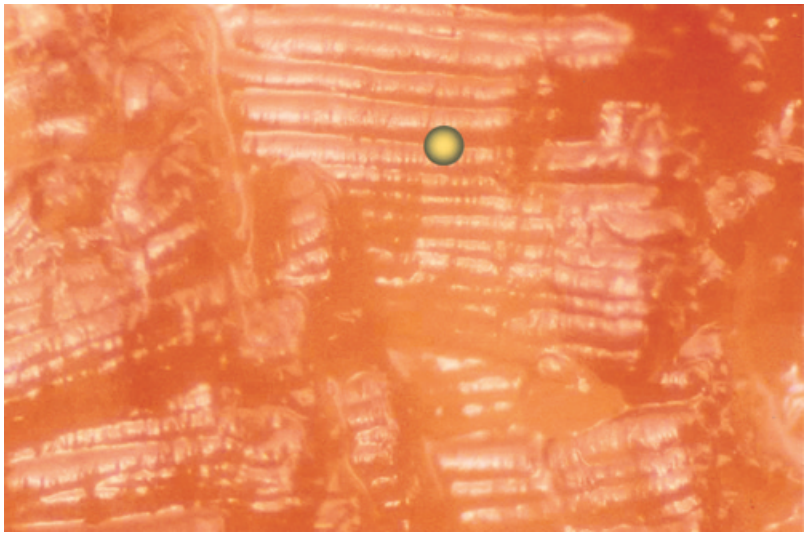

Fig. 4. A close-up image of individual muscle fibers. The internal blood vessels have been removed from a muscle slice (see Fig. 6B) from which a fascicle has been manipulated in order to expose the interfiber spaces. No adipocytes can be detected between the fibers. This is typical for rat muscle. A fat cell of average size is artificially drawn on top of the fibers for presentation purpose, emphasizing the impossibility of the existence of fat cells between the muscle fibers. Original magnification: ~×100.

proximately one-third to one-half of that measured in samples that had not undergone microdissection. The differences were highly significant both statistically (P = 0.01–0.001) and in absolute terms (**Table 1**).

The smaller (distal) blood vessels inside the skeletal muscle samples were difficult to identify and to remove. Thus, we determined the TG content of internal blood vessels in order to estimate the amount of TG associated with these nonremovable small vessels. We found that rat muscle contained <1% (by weight) blood vessels (the major blood vessels that can be identified and removed under a microscope). These major vessels contain <1% TG by weight. Because smaller vessels are associated with far fewer, if any, adipocytes, the TG associated with the nonremovable small vessels are therefore negligible.

NMR studies of muscle TG distribution

Soleus, gastrocnemius, and tibialis anterior muscle samples from lean and obese rats were analyzed by high resolution NMR proton spectroscopy. With this technology, the methylene protons of the fatty acid chains of imcTG produce a chemical shift at 1.3 ppm whereas those of emcTG (e.g., adipocytes in the interfascicular spaces) produce a chemical shift at 1.5 ppm. Liver, which contains only intracellular TG, and subcutaneous fat tissue of rat were used as the standards for intracellular and extracellular lipids, respectively (4). The proton spectra of tissue samples are presented in **Fig. 7**. As expected, the methylene protons of adipose tissue fatty acids appear at 1.5 ppm (Fig. 7A) whereas those of liver TG appear at 1.3 ppm (Fig. 7B). All muscle TG showed up at 1.3 ppm only (Fig. 7D, 7G, and 7I) as a clean, well-resolved peak. No peak

Fig. 5. A major internal blood vessel within a piece of rat gastrocnemius muscle sample ready to be removed. Major blood vessels, such as the one to the right of the exposed one, are highly visible under a stereo microscope and can be easily removed.

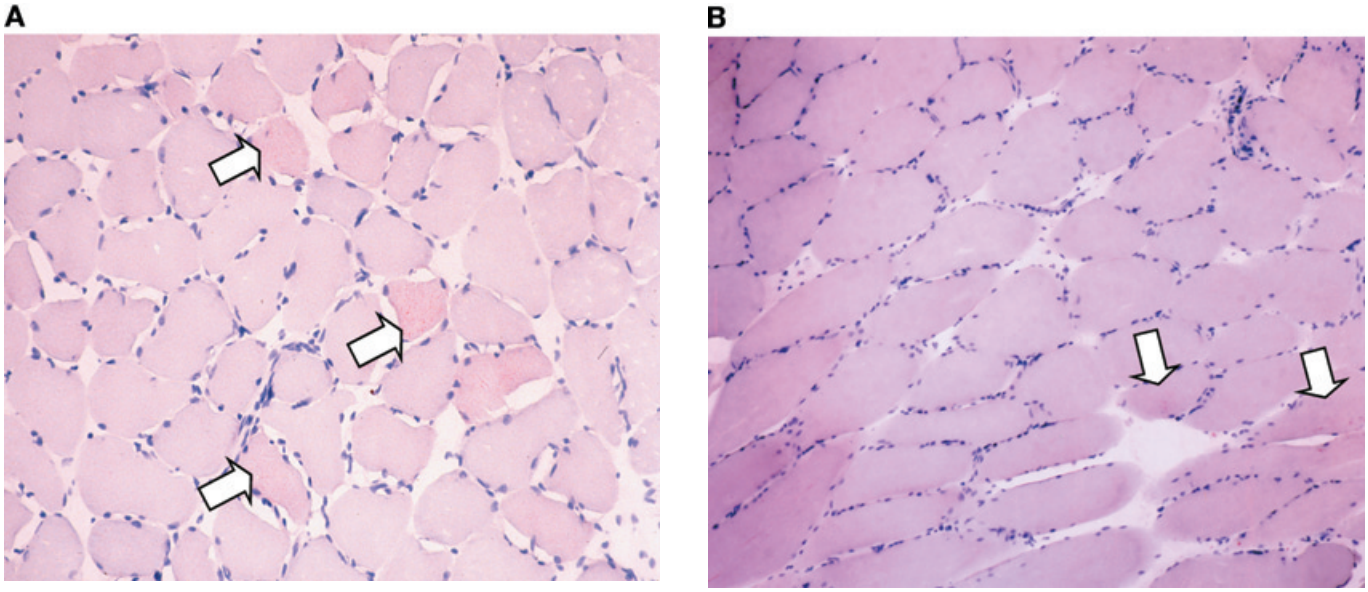

Fig. 6. A: Oil red O staining of a rat soleus muscle fascicle cross-section at 6 μm, viewed under a high resolution light microscope. The image shows the individual muscle fibers. Red stains (TG) are visible in some fibers (arrows). No stains can be seen between the fibers, indicating the absence of extramyocellular adipocytes or TG between fibers. Nuclei appear as dark blue (original magnification: ×150). B: Oil red O staining of a rat gastrocnemius muscle fascicle cross-section. It appears with less red staining (TG) than the soleus as seen in (A) (original magnification: ×300).

was detected at 1.5 ppm from these muscle samples. To test the detection power for extramyocellular adipocytes, 2 mg of rat adipose tissue (the estimated weight of imcTG contained in that particular piece of muscle sample) was added to the tube containing the gastrocnemius sample. The proton spectra then showed a doublet peak at 1.3 ppm (the same peak as seen in Fig. 7D) and 1.5 ppm (from the added fat) (Fig. 7E). After addition of another, larger piece of fat to the same tube, the main proton peak shifted to 1.5 ppm (Fig. 7F), in response to the added fat. The original, smaller peak at 1.3 ppm was completely obscured. Figure 7G and 7H shows similar chemical shifts caused by adding fat tissue to the tibialis anterior muscle sample. A sample of commercial pork with an average degree of marbling (interfascicular adipose tissue) showed a prominent peak at 1.5 ppm, indicating that the TG are mainly in the extramyocellular pool (Fig. 7C). The lower detection limit for triglycerides by NMR proton spectroscopy was estimated to be 10 μM (data not shown) at 100 scans. Thus, the absence of a peak at 1.5 ppm from rat muscle (Fig. 7D, 7G, and 7I) was not due to instrumental limitation but was indeed due to the nonexistence of extramyocellular adipocytes.

Micro-CT analysis of skeletal muscle

Figure 8A (lean rat) and Fig. 8B (obese rat) show two sets of reconstructed global micro-CT images of soleus muscle. Each set of images consists of three views of the muscle from three different angles (front, lateral, and top). No dark, round-shaped spots were visible in the images and therefore it was concluded that no fat cells were present in the muscle samples. Note that to facilitate presentation, the entire length of each muscle sample is not shown.

DISCUSSION

Despite widespread concerns regarding the contamination of intramyocellular lipids by extracellular sources, direct experimental data have been lacking about the de-

TABLE 1. Triglyceride content of rat skeletal muscles before and after removal of extramyocellular adipocytes

Extramyocellular Adipocytes	Body Weight	Muscle TG Content		
		Gastrocnemius	Soleus	Tibialis Anterior
	g	*μmol/g wet weight*		
Dissected[a] (n = 6)	485 ± 10	0.44 ± 0.08	2.22 ± 0.28	0.46 ± 0.07
Not dissected[a] (n = 5)	483 ± 8	1.26 ± 0.16	4.16 ± 0.8	2.05 ± 0.53
P (dissected vs. ND)		0.001	0.01	0.005

[a] The intramuscular (interfascicular, vessel-associated adipocytes) and external adipocytes were either removed (dissected) or not removed (not dissected, ND) before the determination of muscle TG content, using an enzymatic method (see Materials and Methods). The statistical comparisons were unpaired.

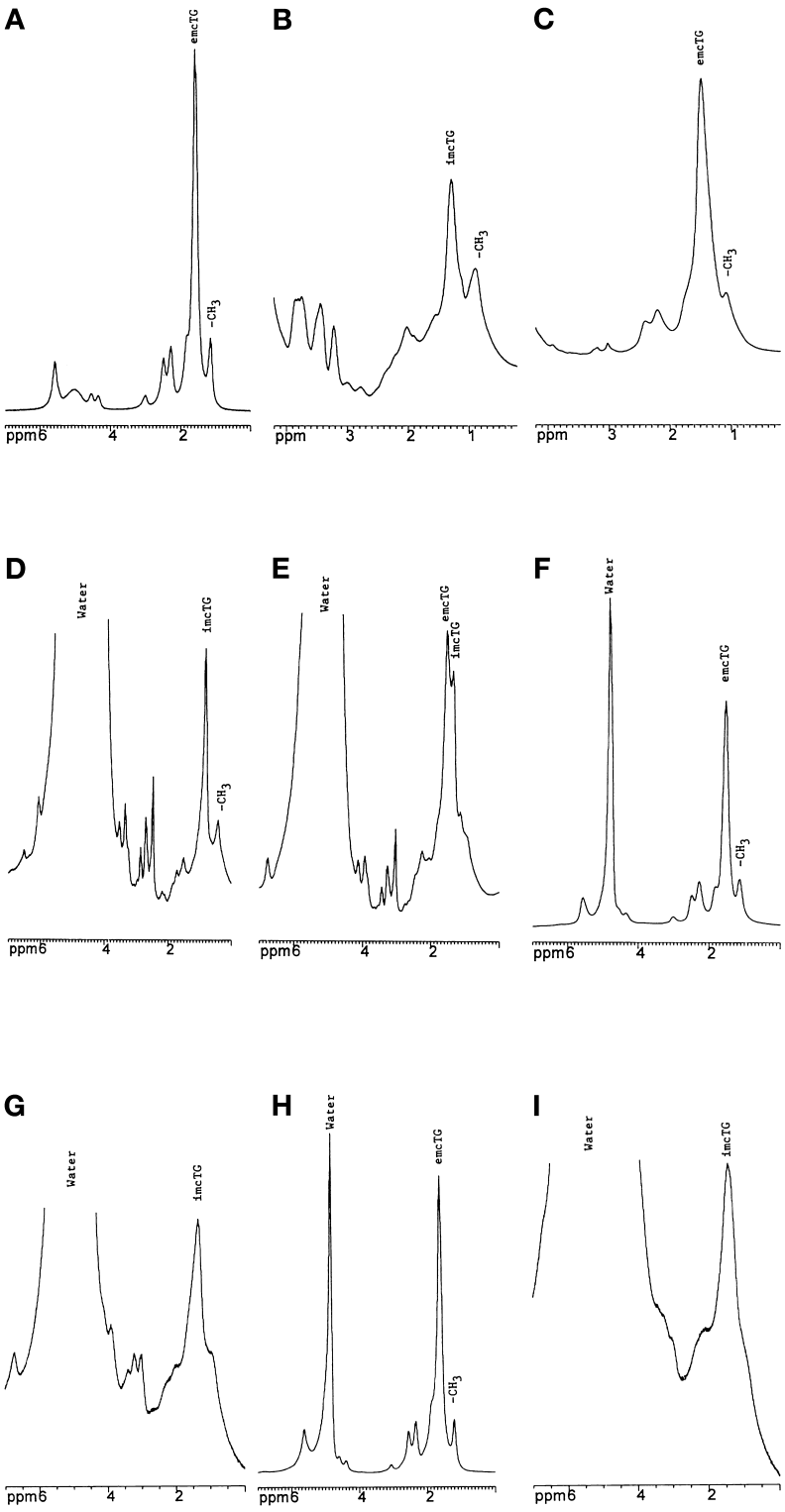

Fig. 7. A: Proton spectrum of rat subcutaneous adipose tissue. The methylene proton signals of the TG fatty acid chains are shown as the largest peak at 1.5 ppm. The assignments are relative to the water peak at 4.8 ppm. Because water is almost absent in fat tissue, its signal has been calibrated with standard sucrose solution and then locked for the analysis. All the analyses were conducted at 500 MHz. B: Proton spectrum of liver from a lean rat as a standard of imcTG (the liver lacks emcTG). The methylene proton signals of the TG fatty acid chains are shown as the largest peak at 1.3 ppm. The assignments are relative to the water peak at 4.88 ppm (the same for samples C–I). C: Proton spectrum of commercial pork with average degree of marbling. The methylene proton signals of the pork TG fatty acid chains are shown at 1.5 ppm, indicating the TG are predominantly in the emcTG pool. Proton signals of imcTG fatty acid chains are obscured by signals from the overwhelming marbling fat. D: Proton spectrum of gastrocnemius muscle from an obese rat. The methylene proton signals of TG fatty acid chains are shown at 1.3 ppm without apparent signals at 1.5 ppm, indicating that the TG are all in the imcTG pool without detectable emcTG. E: Proton spectrum of the same gastrocnemius muscle as in (D), with the addition of 2 mg of subcutaneous fat tissue [the estimated amount of imcTG contained in this particular piece of muscle used in the analysis (9)]. The methylene proton signals are now shown as a doublet: the peak at 1.5 ppm is the signal from the added fat and the peak at 1.3 ppm is the same imcTG signal as seen in (D). F: Proton spectrum of the same samples as in (E) with the addition of more fat tissue. Now the methylene proton signals are almost entirely from the added fat with the signals of imcTG being completely covered because of its small mass. Note the difference in the ratio of the methylene signals to water peak between (F) and (D) and (E). In (F), the methylene signals are many times stronger than those in (D) or (E) because of the addition of a larger piece of fat tissue. G: Proton spectrum of tibialis anterior muscle from an obese rat. The methylene proton signals of TG fatty acid chains are shown at 1.3 ppm, indicating the muscle TG are in the imcTG pool with emcTG undetectable. H: Proton spectrum of the same tibialis anterior muscle sample as in (G) with the addition of a relatively large piece of fat tissue. The methylene proton signals are now at 1.5 ppm, which completely obscured the peak at 1.3 ppm as seen in (G). I: Proton spectrum of soleus muscle from an obese rat. The methylene proton signals of TG fatty acid chains are shown at 1.3 ppm without detectable signals at 1.5 ppm. Note: the 1.3-ppm peak is shifted to 1.4 ppm in this particular analysis.

gree to which extramyocellular fat is present in skeletal muscle, and the feasibility of removing it. Therefore, at present there is no consensus about our ability to sample the true intramyocellular lipid pools, or about the practicality thereof. On the basis of the data from the present study, the presence of adipocytes associated with rat skeletal muscle can be substantial. These extramyocellular lipids are potentially contaminating sources. Without careful microscopic dissection of the muscle samples, the TG from these extramyocellular adipocytes can overwhelm the intramyocellular lipid pools, leading to highly erroneous results in the study of muscle lipid metabolism. This is especially true in obesity, in which state the amount of muscle-associated fat tends to increase. Although interfascicular adipocytes are found to be absent in rat, external adipocytes are often numerous. This is especially true for the soleus, where adipocytes or even fat tissue is usually present on the exterior.

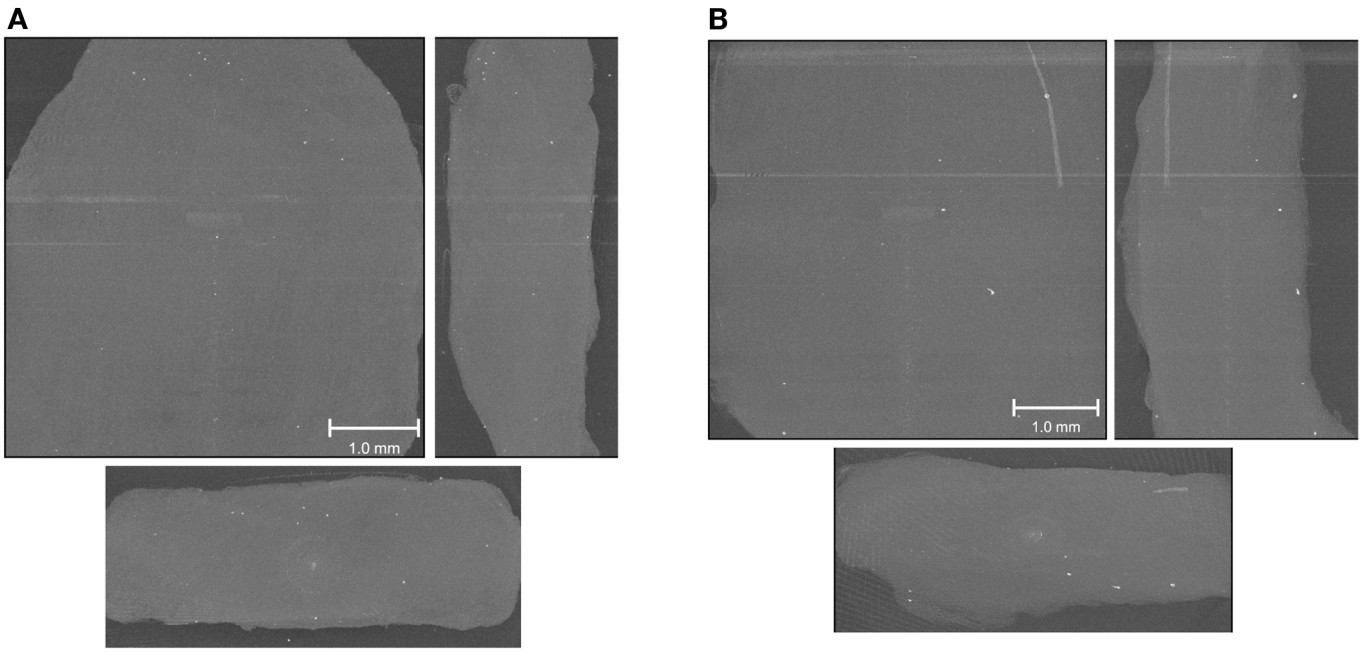

Fig. 8. Reconstructed micro-CT global images of soleus muscle from a lean rat (A) and from an obese rat (B). The three images shown in (A) and (B) are the views from the front (top left), side (top right), and top (bottom) of the muscle. The images were obtained by maximum intensity projection, reconstruction voxel 5.7 μm, display voxel 11.5 μm. None of the images shows the presence of adipocytes within the muscle tissue, which would have appeared as dark, round spots with a diameter of ~100 μm. A positive control of fat cells with X-ray micro-CT was conducted previously and is not included in this particular analysis.

On the other hand, it is encouraging to see that the potentially contaminating extramyocellular lipids can be removed by using appropriate equipment and procedures. Thus, the presence of extramyocellular fat does not constitute an absolute obstacle for sampling the true intramyocellular lipid pool. The essential components of the procedure are *1*) a stereo microscope, *2*) proper surgical instruments, and *3*) sufficient time. The time needed to thoroughly clean up a muscle sample of up to 0.5 g is in the range of 5–15 min, depending on the distribution of the fat and the type of muscle. For example, bulk fat is easy to identify and remove. Scattered adipocytes (e.g., those on the surface of the myotendon junction on the soleus) require more time to locate and to remove. The removal of major internal blood vessels is straightforward because they are highly visible under the microscope. Gastrocnemius and tibialis anterior muscles are easier to process compared with soleus muscle.

The key to the present finding is our direct observation and confirmation that adipocytes are not present between muscle fibers within or between muscle fascicles in healthy muscle tissue, as has been suggested previously (14). Indeed, it seems impossible to imagine that large adipocytes (diameter of 70–110 μm) could exist between muscle fibers (diameter of 75–100 μm) without disrupting the highly organized structure of the muscle fascicles and the constituent fibers (Fig. 4). With the absence of adipocytes in the interstitial space, it becomes relatively easy to remove fat cells from other spaces, such as the exterior surface and the internal blood vessels, to obtain pure muscle fibers. We consider this finding regarding the absence of fat cells in the interstitial space to be significant, in that it assures that obtaining pure muscle fibers is practical. This finding is expected to help remove the widespread, but unsubstantiated doubts about the practicality of sampling the pure imcTG pool for metabolic studies. In comparing the rat muscle imcTG content from the present study with those from previous studies (7), we suspect that less variable and more comparable data may have been obtained if microscopic dissection had been performed in the previous studies. We suggest that this approach be used in future studies involving the sampling of the imcTG pool.

It is important to note that adipocytes on the muscle surface are invisible to the naked eye. These adipocytes must be closely examined and removed under a microscope before proceeding to the interior. The external blood vessels, which are always bigger than the internal vessels and are more often associated with adipocytes, also must be completely removed.

In conclusion, rat skeletal muscle is primarily associated with external adipocytes. In addition, a limited number of adipocytes may exist in association with internal blood vessels. Adipocytes are absent in the interstitial space of skeletal muscle. Both the external and internal adipocytes are removable, but only by microdissection. It is possible and practical to sample the true imcTG pool free of contamination.

This work was supported by grant DK 50456 from the Minnesota Obesity Center to Dr. Z. Guo. The authors thank Dr. M. D. Jensen for suggestions in preparing the manuscript and for support pro-

vided by his grants DK40484, DK45343, and RR-0585 from the U.S. Public Health Service and the Mayo Foundation.

Manuscript received 9 October 2000 and in revised form 20 February 2001.

REFERENCES

1. Koyama, K., G. Chen, Y. Lee, and R. H. Unger. 1997. Tissue triglycerides, insulin resistance, and insulin production: implications for hyperinsulinemia of obesity. *Am. J. Physiol.* **273:** E708–E713.
2. Pan, D. A., S. Lillioja, A. D. Kriketos, M. R. Milner, L. A. Baur, C. Bogardus, A. B. Jenkins, and L. H. Storlien. 1997. Skeletal muscle triglyceride levels are inversely related to insulin action. *Diabetes.* **46:** 983–988.
3. Storlien, L. H., A. B. Jenkins, D. J. Chrisholm, W. S. Pascoe, S. Khouri, and E. W. Kraegen. 1991. Influence of dietary fat composition on development of insulin resistance in rat. *Diabetes.* **40:** 280–289.
4. Szczepaniak, L., E. E. Babcock, F. Schick, R. L. Bobbins, A. Garg, D. Burns, J. D. McGarry, and D. Stein. 1999. Measurement of intracellular triglyceride stores by 1H spectroscopy: validation in vivo. *Am. J. Physiol.* **276:** E977–E989
5. Jacob, S., J. Machann, K. Rett, K. Brechtel, A. Volk, W. Renn, E. Maerker, S. Matthaei, F. Schick, C-D. Claussen, and H-U. Haring. 1999. Association of increased intramyocellular lipid content with insulin resistance in lean nondiabetic offersprings of type 2 diabetic subjects. *Diabetes.* **48:** 1113–1119.
6. Frayn, K., and P. R. Maycock. 1980. Skeletal muscle triacylglycerol in the rat: methods for sampling and measurement and studies of biological variability. *J. Lipid Res.* **21:** 139–144.
7. Gorski, J. 1992. Muscle triglyceride metabolism during exercise. *Can. J. Physiol. Pharmacol.* **70:** 123–131.
8. Russull, J. C., G. Shillabeer, J. Bar-Tana, D. C. W. Lau, M. Richardson, L. M. Wenzel, S. E. Graham, and P. J. Dolphin. 1998. Development of insulin resistance in the JCR:LA-cp rat: role of triacylglycerol and effects of Medica 16. *Diabetes.* **47:** 770–778.
9. Guo, ZK., and M. D. Jensen. 1998. Intramuscular fatty acid metabolism evaluated with stable isotopic tracers. *J. Appl. Physiol.* **84:** 1674–1679.
10. Folch, J., M. Lees, and G. H. Sloane-Standley. 1957. A simple method for the isolation and purification of total lipids from animal tissues. *J. Biol. Chem.* **226:** 497–509.
11. Christie, W. W. 1985. Rapid separation and quantification of lipid classes by high pressure liquid chromatography and mass detection. *J. Lipid Res.* **26:** 507–512.
12. Humphrey, S. M., R. M. Fisher, and K. N. Frayn. 2000. Micromethod for measurement of subnanolole ammounts of triacylglycerol. *Ann. Clin. Biochem.* **27:** 597–598.
13. Jorgensen, S. M., O. Demirkaya, and E. L. Ritman. 1998. Three-dimensional imaging of vasculature and parenchyma in intact rodent organs with X-ray micro-CT. *Am. J. Physiol.* **275:** H1103–H1114.
14. Engel, A. G., and C. Franzini-Armstrong. 1994. Myology. McGraw-Hill, New York. p. 242.